

REPORT DOCUMENTATION PAGE

AD-A269 709



Form Approved
GPO No. 0704-0188

2

estimated to average 1 hour per response, including the time for reviewing instructions, searching existing data sources, gathering and the collection of information. Send comments regarding this burden or any other aspect of this collection of information, including suggestions to the Director for Information Operations and Reports, 1215 Jefferson Davis Highway, Suite 1204, Arlington, VA 22202-4302, and to the Office of Management and Budget, Paperwork Project (0704-0188), Washington, DC 20503.

2. Report Date. August 1993		3. Report Type and Dates Covered. Final - Journal Article	
4. Title and Subtitle. Sensitivity of the deconvolution of acoustic transients to Green's function match		5. Funding Numbers. Program Element No. 0601153N Project No. 3202 Task No. 340 Accession No. DN257015 Work Unit No. 12442C	
6. Author(s). Michael K. Broadhead, Robert L. Field, and James H. Leclere		8. Performing Organization Report Number. JA 244:064:92	
7. Performing Organization Name(s) and Address(es). Naval Research Laboratory Ocean Acoustics Branch Stennis Space Center, MS 39529-5004		10. Sponsoring/Monitoring Agency Report Number. JA 244:064:92	
9. Sponsoring/Monitoring Agency Name(s) and Address(es). Naval Research Laboratory Center for Environmental Acoustics Stennis Space Center, MS 39529-5004		11. Supplementary Notes. Published in J. Acoust. Soc. Am. 94 (2), Pt. 1.	
12a. Distribution/Availability Statement. Approved for public release; distribution is unlimited.		12b. Distribution Code.	
13. Abstract (Maximum 200 words). In this paper various measurements of acoustic time series recorded in the Atlantic over source-to-receiver ranges of 600 to 12 900 m are analyzed. The transmitted source signature with a monitor hydrophone mounted on the source array was also recorded. The signature distortion introduced by propagation effects was treated by the use of single-channel deconvolution. In situations where the Green's function structure is simple (e.g., direct arrival and surface reflection), single-channel deconvolution gave satisfactory results. When multipath effects (due to interaction with layered bottom sediments) were present, it was difficult to get a good source estimate. A way was developed of perturbing the Green's functions such that the source estimates were guaranteed to improve. In most cases it was found that very small changes could produce significant improvement in the source estimates. This sensitivity was quantified by using the correlation coefficient. This sensitivity is not to be confused with the well-known fact that the single channel deconvolution problem is ill-posed. That issue was treated separately.			
14. Subject Terms. Transients, distributed sensors coherence, detection, classification		15. Number of Pages. 9	
		16. Price Code.	
17. Security Classification of Report. Unclassified	18. Security Classification of This Page. Unclassified	19. Security Classification of Abstract. Unclassified	20. Limitation of Abstract. SAR

DTIC
SELECTE
SEP 23 1993
S B D

**Best
Available
Copy**

Sensitivity of the deconvolution of acoustic transients to Green's function mismatch

Michael K. Broadhead, Robert L. Field, and James H. Leclere
Naval Research Laboratory, Stennis Space Center, Mississippi 39529

(Received 13 July 1992, revised 22 March 1993; accepted 22 April 1993)

In this paper various measurements of acoustic time series recorded in the Atlantic over source-to-receiver ranges of 600 to 12 900 m are analyzed. The transmitted source signature with a monitor hydrophone mounted on the source array was also recorded. The signature distortion introduced by propagation effects was treated by the use of single-channel deconvolution. In situations where the Green's function structure is simple (e.g., direct arrival and surface reflection), single-channel deconvolution gave satisfactory results. When multipath effects (due to interaction with layered bottom sediments) were present, it was difficult to get a good source estimate. A way was developed of perturbing the Green's functions such that the source estimates were guaranteed to improve. In most cases it was found that very small changes could produce significant improvement in the source estimates. This sensitivity was quantified by using the correlation coefficient. This sensitivity is not to be confused with the well-known fact that the single-channel deconvolution problem is ill-posed. That issue was treated separately.

PACS numbers: 43.30.Wi

INTRODUCTION

Acoustic transients are signals that typically have broadband spectra and a well-defined time duration, as opposed to, say, the persistent, narrow-band signature of a propeller blade. Sources of underwater acoustic transients include man-made devices, sounds produced by natural phenomena such as ice shifting or breaking, and biologic sounds such as those produced by whales and other sea life.

The problem of determining the nature of a transient sound source, or the classification problem, is currently of interest to the underwater sound community. Much of the effort to date has centered on the problem of signals that have not been distorted by propagation through the environment. Propagation effects (or environmental distortion) include attenuation and multipath effects. In this study, we will confine ourselves to low frequency (< 150 Hz) phenomena, so we will expect most of the attenuation to occur due to bottom interaction. Since we are dealing with relatively short ranges, we will mainly be concerned with multipath effects. One approach to classification in the presence of environmental distortion effects is to first calculate the propagation effects, and then remove them in a signal processing step. The output would then be an estimate of the transient source signature that could be used as input into any one of a number of classification (pattern recognition) schemes. We can account for propagation effects by computing the Green's function $G(\mathbf{r}, t; \mathbf{r}', t')$. For a point source at \mathbf{r}' and a receiver at \mathbf{r} , the processing step requires deconvolving the pressure time series $\psi(\mathbf{r}, t)$ with $G(\mathbf{r}, t; \mathbf{r}', t')$ for the desired source signature $S(t)$. This involves solving the following Fredholm integral equation of the first kind:

$$\psi(\mathbf{r}, t) = \int_{-\infty}^{+\infty} G(\mathbf{r}, t; \mathbf{r}', t') S(t') dt', \quad (1)$$

where \mathbf{r} and \mathbf{r}' are fixed for a given case. It is well known that this problem (single-channel deconvolution) is ill-posed.^{1,2} This is a different type of sensitivity from the kind we are studying, and we will return to this issue later.

A reasonable question to ask is, how accurately does the Green's function have to be computed for the deconvolution to be successful? The information that determines the Green's function includes source and receiver locations, the sound speed and density profiles of the water layer, bottom topography, and the sediment layer parameters (velocity, density, and attenuation profiles). If these environmental parameters are not known to sufficient accuracy and spatial resolution, there will be errors (mismatch) in the Green's function. The practical issue then becomes, how sensitively does the source signature deconvolution problem (actually, its well-posed extension) depend on $G(\mathbf{r}, t; \mathbf{r}', t')$?

The work reported here contributes to the study of these issues by using high SNR experimental data in moderate water depth (915 m), for the low-frequency case, in a mid to short range scenario (600 m–13 km), in which the subbottom sediment layers played an important role in the multipath structure. We performed a sensitivity analysis on the deconvolution of the data with computed Green's functions using the best available geoacoustic information. This study was part of a larger effort to analyze these data while simultaneously evaluating a (then) new propagation model.³

We proceeded with the sensitivity analysis by deconvolving the data with computed Green's functions and then perturbing the Green's functions in such a way that the source estimates would be guaranteed to improve. We then used the correlation coefficient measure to show that significant increases in deconvolution quality were gained from small changes (usually) to the calculated Green's function. This leads us to suspect that the geoacoustic pa-

93-22062



1993

8

8

8

8

8

8

8

8

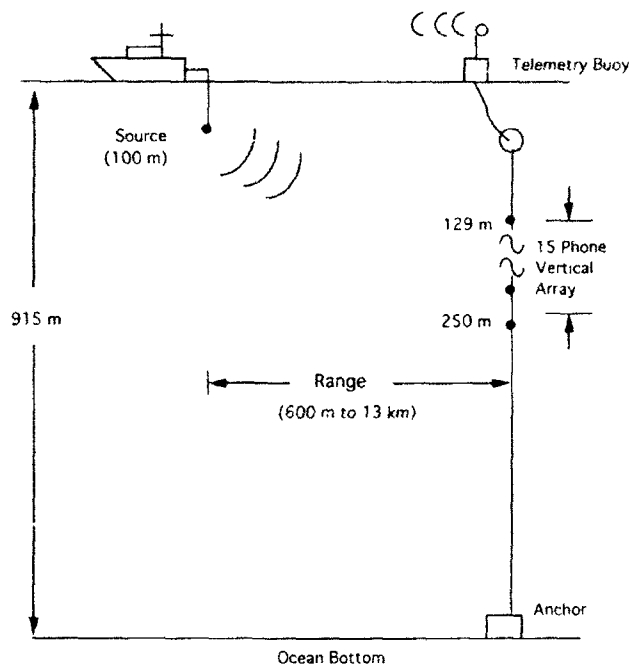


FIG. 1. Experiment geometry. Location—Blake Plateau; water depth—915 m; source—HLF-2AH towed source; bandwidth—25- to 150-Hz linear sweep; array—15-element vertical array.

Parameters and source location may need to be known to a greater accuracy than will be feasible, at least in environments where the multipath structure becomes sufficiently complex.

In the rest of this paper we will describe the data set we have worked with, the modeling that was done, and the initial deconvolution results using the model Green's function. We will then present the optimization method that will allow us to perturb the model Green's function to get better deconvolution results, and show results from calculations with the data. Finally we will summarize our results and present some conclusions.

I. EXPERIMENT DESCRIPTION

The experiment from which our data were obtained was conducted in the vicinity of 27.5°N, 78.3°W (Blake Plateau) in the Atlantic Ocean (see Fig. 1). The water bottom was fairly smooth and the water depth was approximately 915 m. The experiment included measurements using a 25- to 150-Hz linear sweep pulse produced by an HLF-2AH towed acoustic source. The signals were recorded on a stationary 15-element vertical line array with 9-m hydrophone spacing. The top hydrophone was at a depth of $Z=129$ m and the bottom hydrophone was at $Z=250$ m. Refer to Field and Leclere³ for more detail.

II. DATA PREPARATION AND MODELING

In Fig. 2 we display the (correlated) time series for the five source-to-receiver ranges (R), 600, 1500, 4300, 7900, and 12 900 m. The hydrophone depth is $Z=129$ m. These data have been cross correlated with the measured source signature from a monitor hydrophone to improve the SNR.

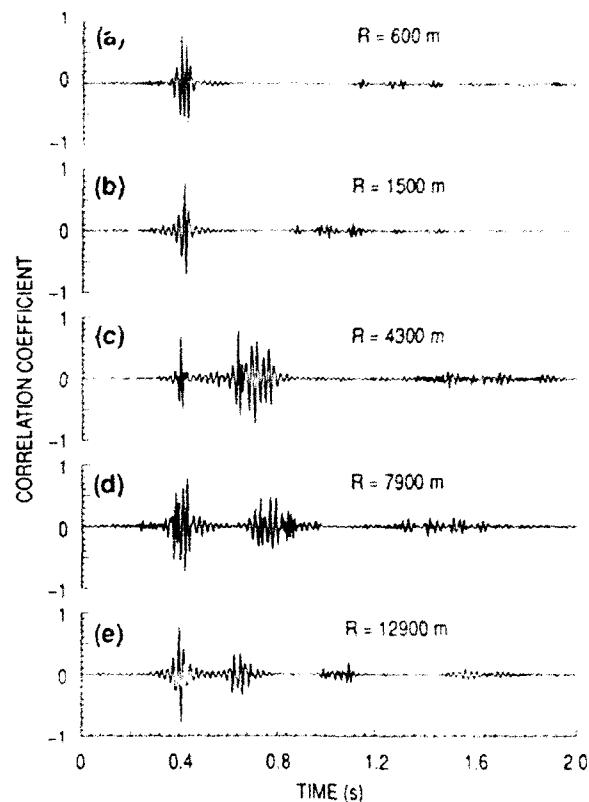


FIG. 2. Measured transmissions at receiver depth $Z=129$ m for the five ranges considered. Data have been correlated with the measured source signature.

In the $R=600$ m and $R=1500$ m cases, the arrival structure is primarily composed of direct arrival and surface bounce. There are some low amplitude bottom interactions past 0.8 s. However, in the other three cases, $R=4.3$, 7.9, and 12.9 km, there is significant bottom interaction present, which plays an important role in this study (refer to Field and Leclere³). In Fig. 3 we show the (correlated) measured source signature. This quantity plays the role of $S(t)$ in our calculations. It is also the ground truth or standard by which our source estimates will be judged. In Fig. 4, we display the computed model Green's functions

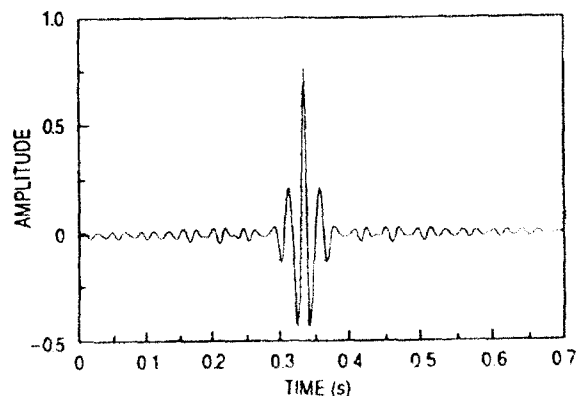


FIG. 3. The source signature (after correlation) that was transmitted (measured from a monitor hydrophone).

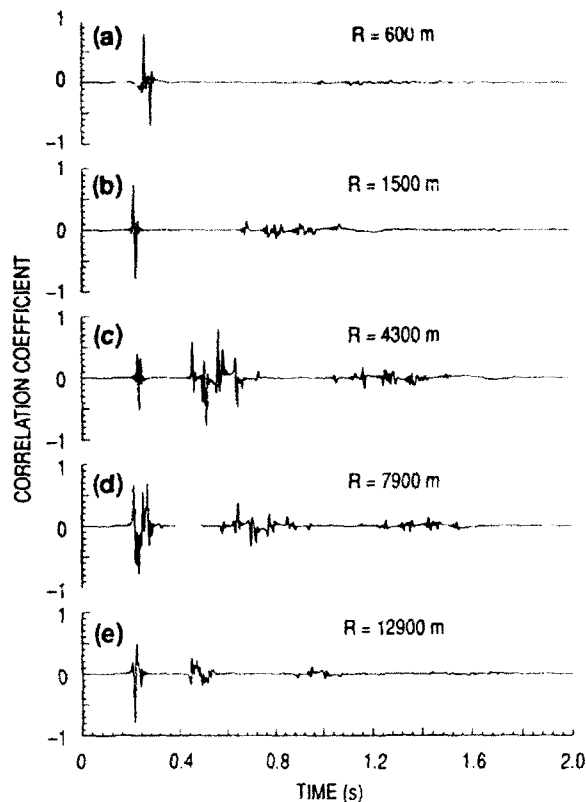


FIG. 4. Computed (TDPE) band-limited Green's functions for the 129-m hydrophone.

for the corresponding measurements. The model used was the time domain parabolic equation (TDPE) model.^{4,5} Bathythermographs were used to obtain water column sound speeds while sediment velocities and densities were extrapolated from data gathered at Deep Sea Drilling Project sites near the experiment. These environmental parameters were input into TDPE along with a desired source-to-receiver range, producing a band-limited (0 to 150-Hz) Green's function as output. Refer to Field and Leclere³ for more detail.

In Fig. 5 we show the simulations produced by convolving the source $S(t)$ in Fig. 3 with the Green's functions in Fig. 4. The simulations are overlaid (dashed) with the measurements (solid) in Fig. 2. For a quantitative comparison, note the correlation coefficients (γ) that are provided. γ is defined in the usual way so that $|\gamma| \leq 1$, where

$$\gamma = \frac{\sum_i [(x_i - x_\mu)(y_i - y_\mu)]}{\sqrt{\sum_i x_i^2 \sum_i y_i^2}}, \quad (2)$$

and x_μ, y_μ are means. Notice that for $R = 600$ m, $\gamma = 0.883$ and for $R = 1500$ m, $\gamma = 0.827$. This demonstrates that the model, environmental input, and the various assumptions made are all reasonable for at least some cases. However, for $R > 4.3$ km, the simulation does not match the data as well ($\gamma < 0.638$). This is presumed to be at least partly due to the fact that significant bottom interaction is present. The bottom interaction presents a problem because we

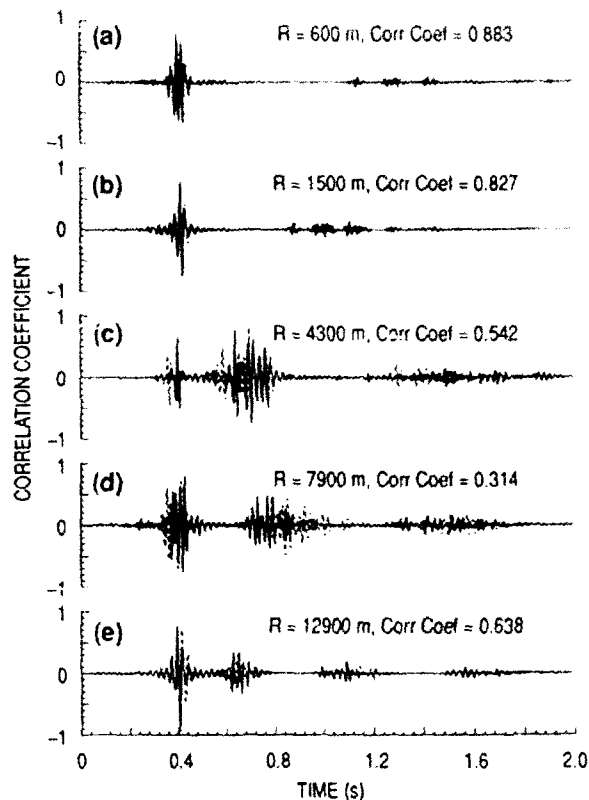


FIG. 5. Measurements in Fig. 2 (solid) compared with simulations (dashed) produced by convolving source signature in Fig. 3 with Green's functions in Fig. 4. The correlation coefficient provides a quantitative comparison.

have limited information on the sediment layer geophysical parameters.

III. DECONVOLUTION ALGORITHM AND RESULTS

As mentioned earlier, the importance of the Green's function from the point of view of the transient classification problem is that it gives us, along with the received signal, enough information to solve Eq. (1) for the source signature $S(t)$. We will present some deconvolution results, but first we will discuss some of the theoretical and computational aspects. We have already pointed out that the deconvolution problem represented by Eq. (1) is mathematically ill-posed. Exactly what does this mean? According to Tikhonov and Arsenin¹ and Tarantola:²

Definition 1: If a solution $S(t)$ exists, is unique, and is a continuous function of the initial data $\psi(r, t)$, then the problem is well-posed. Otherwise, it is ill-posed.

Definition 2: Small changes in the initial data $\psi(r, t)$ yield arbitrarily large changes in the solution $S(t)$.

Tikhonov and Arsenin¹ point out that, in practice, many mathematical problems of physical interest are ill-posed. They and others have published techniques for providing well-posed extensions of these problems. Tikhonov regularization,^{1,6} pre-whitening,⁷⁻⁹ and singular value decomposition (SVD)^{2,10} are some examples. Before we proceed further with this discussion, it will be useful for us to

recast Eq. (1) in a discrete form that is amenable to computer implementation.

Let R and Z be fixed. Then the discrete (computed) Green's function can be written as a column vector $\mathbf{g}=[g_1, g_2, g_3, \dots]^T$, where the subscript indexes time samples. We can also write this discrete Green's function in a convolutional matrix form,¹¹

$$\mathbf{G} = \begin{pmatrix} g_1 & 0 & 0 & \dots \\ g_2 & g_1 & 0 & \dots \\ g_3 & g_2 & g_1 & \dots \\ g_4 & g_3 & g_2 & \dots \\ \dots & \dots & \dots & \dots \end{pmatrix}. \quad (3)$$

If \mathbf{s}_e is the column vector for the unknown source estimate and \mathbf{d} is the data vector for our choice of R and Z , then the discrete form of the convolution equation can be written,

$$\mathbf{G}\mathbf{s}_e = \mathbf{d}. \quad (4)$$

As is well known, this linear system is over determined and may have no solution.¹¹ A common approach to constructing a solution is to use the method of least squares. We define an error vector \mathbf{e} as

$$\mathbf{e} \equiv \mathbf{G}\mathbf{s}_e - \mathbf{d}. \quad (5)$$

We then seek \mathbf{s}_e so that the square length $\mathbf{e}^T\mathbf{e}$ is a minimum. The normal equations obtained from setting the gradient to zero are

$$\mathbf{G}^T\mathbf{G}\mathbf{s}_e = \mathbf{G}^T\mathbf{d}. \quad (6)$$

This linear system is evenly determined but may be ill-conditioned. This is the matrix version of the fact that the original integral equation was ill-posed. In order to provide a well-posed extension, we chose the method of pre-whitening, which has been shown⁷ to be a form of Tikhonov regularization.^{1,6} We initially used SVD, but found the extra computational burden unnecessary. The form of the normal equations with pre-whitening are

$$(\mathbf{G}^T\mathbf{G} + \lambda\mathbf{I})\mathbf{s} = \mathbf{G}^T\mathbf{d}, \quad (7)$$

where $\lambda = \epsilon\phi_0$, ϕ_0 is the main diagonal element (they are all the same), ϵ is a small positive number, and \mathbf{I} is the identity matrix. The idea behind pre-whitening is that it prevents any eigenvalues of the coefficient matrix from becoming too small by giving them all a positive shift. Here, λ can also be interpreted as a Lagrange multiplier for the addition of a finite filter energy constraint.^{7,8} Since the normal equations have a Toeplitz structure,¹² we were able to use the efficient Levinson recursion method for solution.^{12,13} As a further processing step, we applied a hi-cut filter to preserve only the original Green's function bandwidth.

In Fig. 6 we have displayed the results of deconvolving the five measurements in Fig. 2 with the Green's functions in Fig. 4. The results are the dashed plots and are overlaid with the measured source signature (solid) that was previously shown in Fig. 3. We have provided the correlation coefficients for a quantitative comparison. Note that they

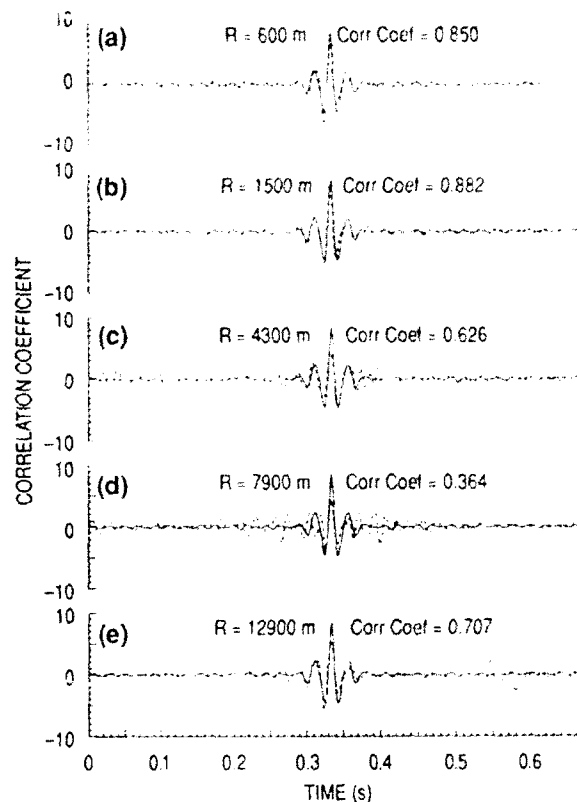


FIG. 6. Source signature (solid) compared with source estimate (dashed) produced by deconvolving measurements in Fig. 2 with Green's functions in Fig. 4.

are comparable to the correlation coefficients in Fig. 5, where we compare simulations and measurements. We will see the close connection between these two quantities again in this paper. It is not surprising that the match between the simulations $S(t)*G(t)$ ($*$ means convolution) and the data are a good predictor of the quality of the deconvolutions. We should point out that the source estimates for $R=600$ m and $R=1500$ m are probably of a "usable" quality in a classification sense; $R=12.9$ km may be marginally usable; $R=4300$ and 7900 m are probably not usable. So, a simple fall off in quality with range is not a justified conclusion.

IV. MISMATCH PROBLEM AND SOLUTION

It was of interest for us to determine how much the environmental parameters would have to change to produce correlation coefficients that were comparable to the $R=600$ m and $R=1500$ m cases. To solve this problem directly was computationally prohibitive in terms of the resources available. As an alternative, we chose to perturb only the Green's function itself, instead of the environmental parameters the Green's function is calculated from.

In order to perturb the Green's function in a meaningful way, we set up a double objective optimization problem, i.e., one with two goals. If our current $G(t)$ (where we have fixed \mathbf{r} and \mathbf{r}') does not produce a simulation $S(t)*G(t)$ with good correlation to the measured data, then we seek a new $G'(t)$ that does. However, we do not

want $G'(t)$ to be too different from $G(t)$, which is our tie to the physics of the problem. In other words, we do not want $G'(t)$ to be arbitrary. The problem was set up in the following way: for some fixed R and Z , let the column vector g be the perturbed Green's function we are seeking and let g_M be the model calculated Green's function. Let S be the matrix convolutional form representing the discrete source signature. Recall that d is the correlated measurements vector at range R and hydrophone depth Z . Then the mismatch (or difference) between the perturbed simulation and the measured data will be

$$e_1 = Sg - d. \quad (8)$$

The mismatch between the perturbed Green's function and the model Green's function will be

$$e_2 = g - g_M. \quad (9)$$

Since we wish to see how much it is possible to reduce the mismatch, we need a quantity that measures the sizes of these vectors. Again we choose the least squares criteria. We seek a g to minimize the functional:

$$E(g) = e_1^T e_1 + \beta^2 e_2^T e_2. \quad (10)$$

According to Scales,¹⁴ a quadratic form can be written as,

$$F(x) = \frac{1}{2} x^T A x + b^T x + c, \quad (11)$$

and its gradient can be written,

$$\nabla F(x) = A x + b. \quad (12)$$

If we substitute Eqs. (8) and (9) into Eq. (10), and rearrange terms we get

$$E(g) = \frac{1}{2} g^T [2S^T S + 2\beta^2 I] g + [-S^T d - \beta^2 g_M]^T g + c. \quad (13)$$

Comparing (13) to (11), and then using (12) we can write

$$\nabla E(g) = 2[S^T S + \beta^2 I] g + [-S^T d - \beta^2 g_M]. \quad (14)$$

Upon setting the gradient to zero, we have the normal equations;

$$(S^T S + \beta^2 I) g = \frac{1}{2} (S^T d + \beta^2 g_M). \quad (15)$$

This system was also solved using Levinson recursion. Comparison of Eq. (15) with Eq. (7) shows how β^2 plays a role similar to λ . Although we also used pre-whitening in our numerical solution of (15), it turned out to be needed only when β^2 was zero (or sufficiently small).

Let us briefly examine what the functional in Eq. (10) means. If we consider just the first term alone, then the problem becomes one of finding a g that, under convolution with the source, produces a good match to the measurements (in a least-squares sense). If we consider just the second term alone, the problem is that of finding a g that is most similar to g_M . This problem has the trivial solution $g = g_M$. When we put the two terms together, however, we find we have a double objective optimization problem. If the goals are conflicting, the solution will be a compromise. The term that receives the most emphasis in the compromise is governed by the trade-off parameter β^2 . As β approaches infinity, g approaches g_M . As β approaches 0, g

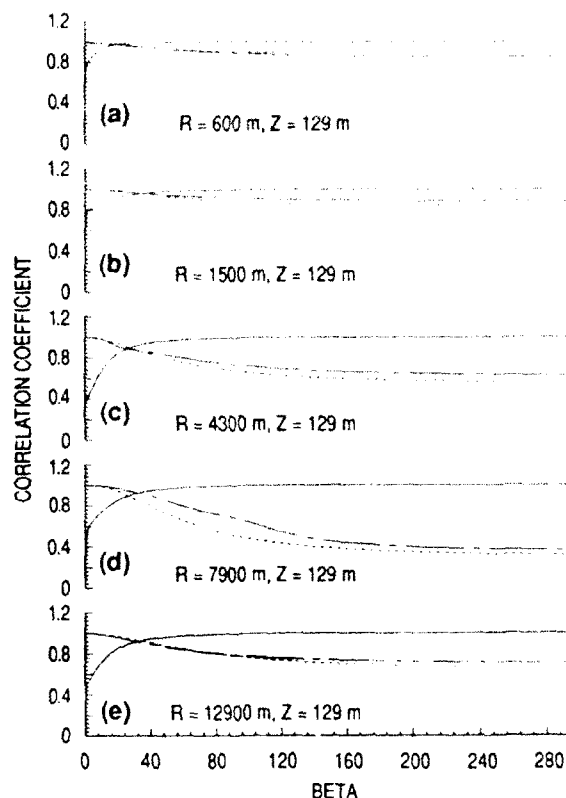


FIG. 7. Beta versus correlation coefficients between the TDPE model Green's functions and the optimized Green's functions (solid); the model simulations and the optimized simulations (dashed); and the source signature and the optimized source estimates from deconvolution (long dash).

approaches the unconstrained deconvolution solution. Another way to view Eq. (10) is that we are adding a constraint that g be close to g_M .

V. OPTIMIZATION RESULTS

In Fig. 7, we show a summary of results from the double objective problem. For a particular R and Z , and a particular β value, the quantity g was produced by solving the linear system in Eq. (15). This "optimized" Green's function was then convolved with s to produce a simulation of the correlated data and was used to deconvolve d to produce a source estimate s_e . The correlation coefficients between the model and optimized Green's function (solid), the measured data and the optimized simulation of the data (dashed), and the source signature and the optimized source estimate from deconvolution (long dash) are then plotted against β . These curves, for each of the five ranges considered, are shown in Fig. 7. We can immediately see several things. First, as noted earlier, simulation quality and deconvolution quality generally follow one another closely. The exception is $R = 7900$, for $40 < \beta < 120$. Second, as expected, the simulation and deconvolution quality increase as g is allowed to depart from g_M . This effect is more pronounced for the last three ranges than for the first two. For $\beta > 300$, β is effectively ∞ , and $g = g_M$.

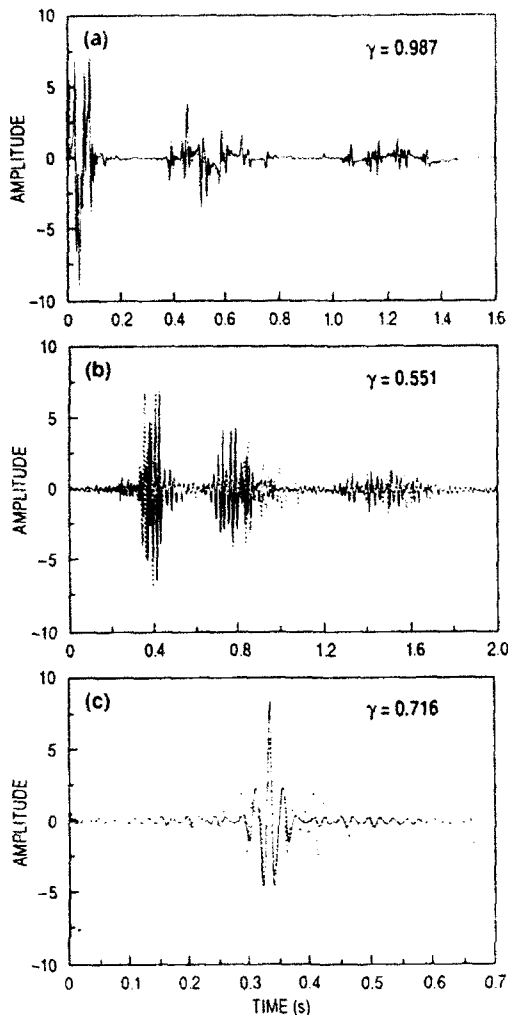


FIG. 8. For $\beta=80$, $R=7900$ m, and $Z=129$ m we have: (a) comparison of model Green's function (solid) and optimized Green's function (dashed), $\gamma=0.987$; (b) comparison of measured data with optimized simulation, $\gamma=0.551$; and (c) comparison of source signature with source estimate obtained by deconvolution of measurement with the optimized Green's function, $\gamma=0.716$.

We take particular note of the crossover point in the curves, which occurs at an average value of $\beta \approx 29$. We have essentially already seen the results for $\beta \geq 300$, so we will pick three interesting β values for a particular range and look at them in more detail. Because the most improvement was gained for $R=7900$ m, we will use this range. For reasons we will explain, we will display the results for $\beta=80$, $\beta=29$, $\beta=0$.

Let us now consider Fig. 8. In Fig. 8(a), we display the model (solid) and optimized (dashed) Green's functions for $R=7900$ m, $Z=129$ m, and a value of $\beta=80$. Notice that the departure of g from g_M is very slight. This is quantified by the correlation coefficient value of $\gamma=0.987$. The simulation produced by convolving g with s is shown in Fig. 8(b). Here, the correlation has improved from a value of $\gamma=0.314$ (refer to Fig. 5) to a value of $\gamma=0.551$. Finally, the deconvolution produced source estimate is shown in Fig. 8(c) [overlaid with the source signature (solid)]. Compare this to the $R=7900$ m case in

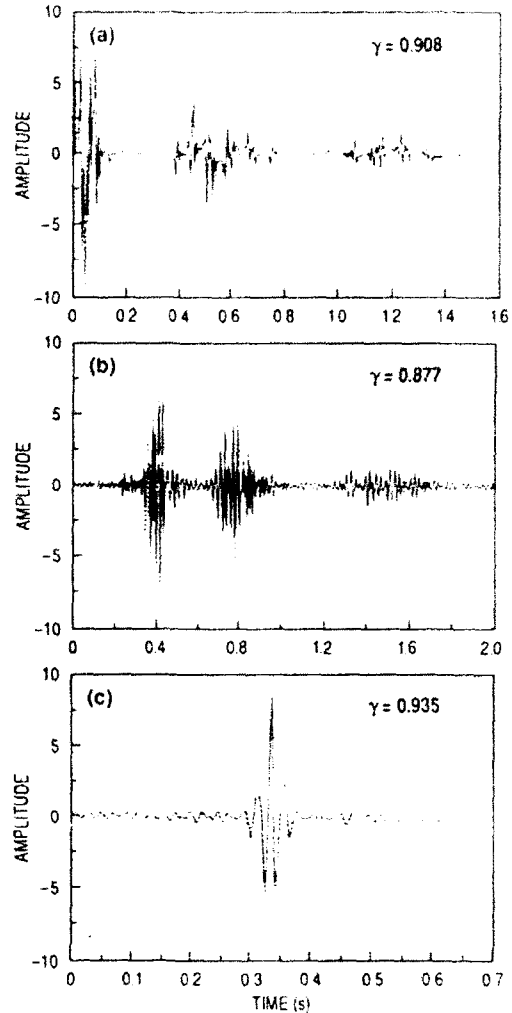


FIG. 9. For $\beta=29$, $R=7900$ m, and $Z=129$ m we have: (a) comparison of model Green's function (solid) and optimized Green's function (dashed), $\gamma=0.908$; (b) comparison of measured data with optimized simulation, $\gamma=0.877$; and (c) comparison of source signature with source estimate obtained by deconvolution of measurement with the optimized Green's function, $\gamma=0.935$.

Fig. 6. The source estimate quality has increased from a value of $\gamma=0.364$ to a value of $\gamma=0.716$. The reason we displayed the $\beta=80$ case was that we have somewhat subjectively picked $\gamma=0.7$ as a cutoff point in a source estimate being usable in a classification sense. Thus, $\beta=80$ allows us to investigate the marginal case.

The significance of $\beta=29$ is, we recall, that it is the crossover value. This means that about equal weight is being given to both terms in the optimization problem. In Fig. 9(a), we show the g vs g_M , with $\gamma=0.908$. Here, the departure is more pronounced, but the two quantities are still very similar. Notice that some of the amplitudes and delays of the impulses have changed slightly. This is the sort of perturbation we would expect for a slight change in geometry (R and Z) or environmental parameters (e.g., water column or bottom sediment layer sound speeds). In Fig. 9(b) we show the simulation comparison. Here, $\gamma=0.877$, which should lead us to expect a good deconvolution. Indeed, in Fig. 9(c), we see that the source estimate

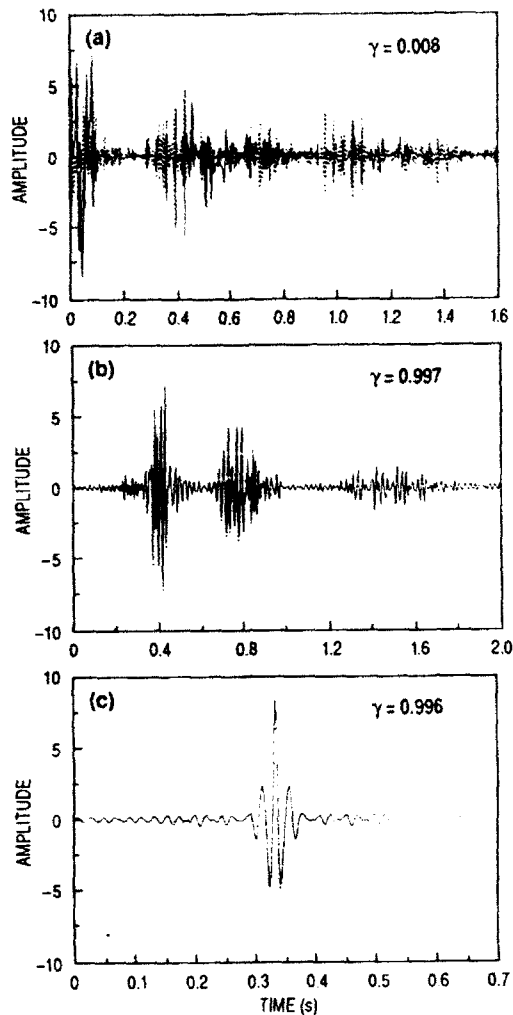


FIG. 10. For $\beta=0$, $R=7900$ m, and $Z=129$ m we have: (a) comparison of model Green's function (solid) and optimized Green's function (dashed) $\gamma=0.008$; (b) comparison of measured data with optimized simulation, $\gamma=0.997$; and (c) comparison of source signature with source estimate obtained by deconvolution of measurement with the optimized Green's function, $\gamma=0.996$.

is quite good, with a value of $\gamma=0.935$. The significance of β is that it is not the best we can do on the simulation and deconvolution, but that it represents about the best we can do without letting g change too much with respect to g_M . To demonstrate this in a more quantitative way, let's look at another extreme, namely, $\beta=0$. In Fig. 10(a), we show the g (dashed) produced by the requirement that under convolution, it should be the best possible match to the data (i.e., $\beta=0$). There is virtually no correlation between it and g_M , i.e., $\gamma=0.008$. In Fig. 10(b), we see that the simulation is almost perfect, with $\gamma=0.997$; and in Fig. 10(c) we have an almost perfect source estimate, with $\gamma=0.996$.

Having established the usefulness of $\beta=29$, let us now go back and look at that case for all five ranges. In Fig. 11, we display the model Green's functions (solid) versus the optimized functions (dashed) for the five ranges considered, along with the corresponding correlation coefficients. The significant feature to notice is that the γ values are all

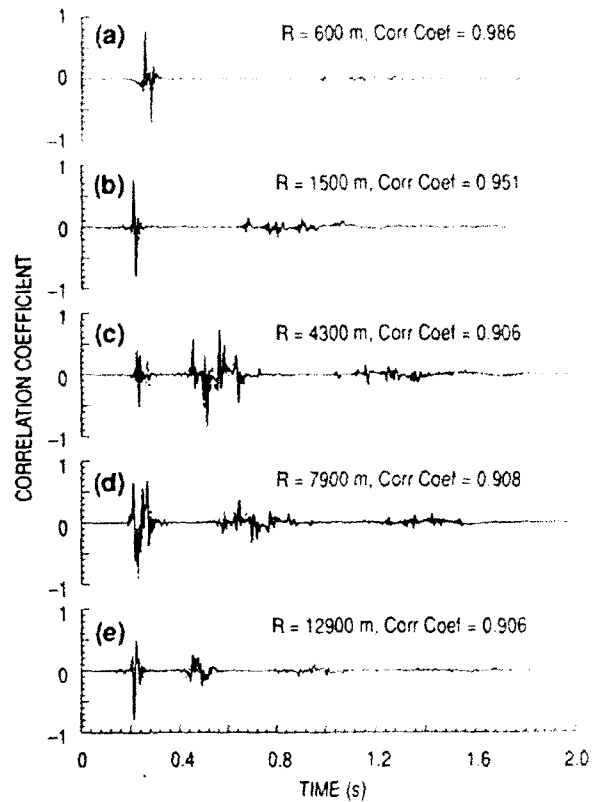


FIG. 11. Comparison of model Green's functions (solid) with optimized Green's functions (dashed) ($\beta=29$) for the five ranges considered.

quite high (in the 0.9's). This means we have done very little perturbing. Now, in Fig. 12, we display the corresponding simulations (cf. Fig. 11). Notice that here also the γ values are quite good. Finally, in Fig. 13, we have the source estimate (cf. Fig. 6). The source estimates are all very good, with γ values mostly in the 0.9's.

In Fig. 14 we summarize the foregoing results by graphing the change in correlation coefficient between $\beta=\infty$ and $\beta=29$ for the g 's, the simulations, and the source estimates for each of the five ranges considered (here, numbered 1 through 5). This figure summarizes in a succinct and quantitative manner the results we have described above. For example, notice that deconvolution quality and simulation quality track well. Also, the first two ranges did not show much change, but the last three did (being of poor quality to begin with). The main point of this figure is that the change in γ for g with respect to g_M , was never very much (<0.1), whereas the corresponding $\Delta\gamma$'s for the source estimates and simulations were considerable (~ 0.6). This has led us to suggest that there is a sensitivity to the exact structure of an impulsive type Green's functions when significant multipath is involved. This idea would have potentially significant impact for the transients classification problem.

VI. SUMMARY

To summarize the evidence for sensitivity in a more succinct way, we can display the means and the maxima

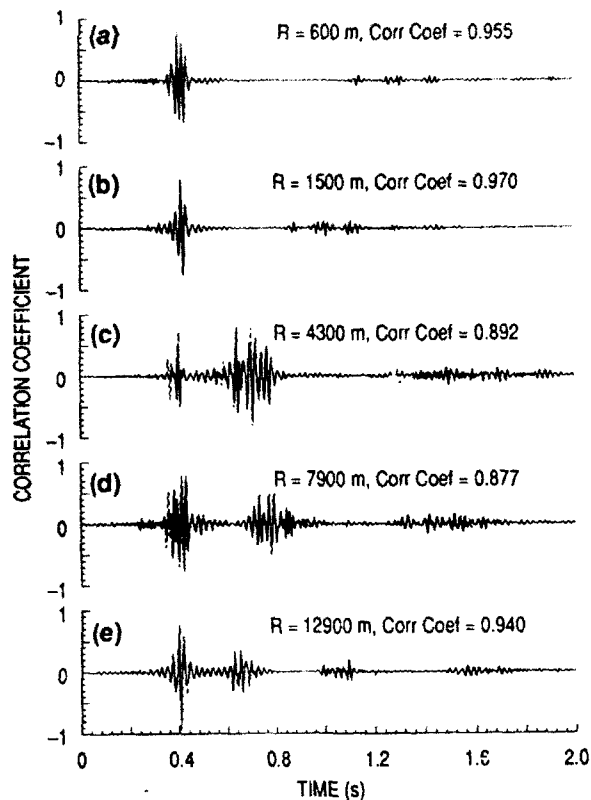


FIG. 12. Comparison of measurements (solid) with optimized simulations (dashed) ($\beta=29$) for the five ranges considered.

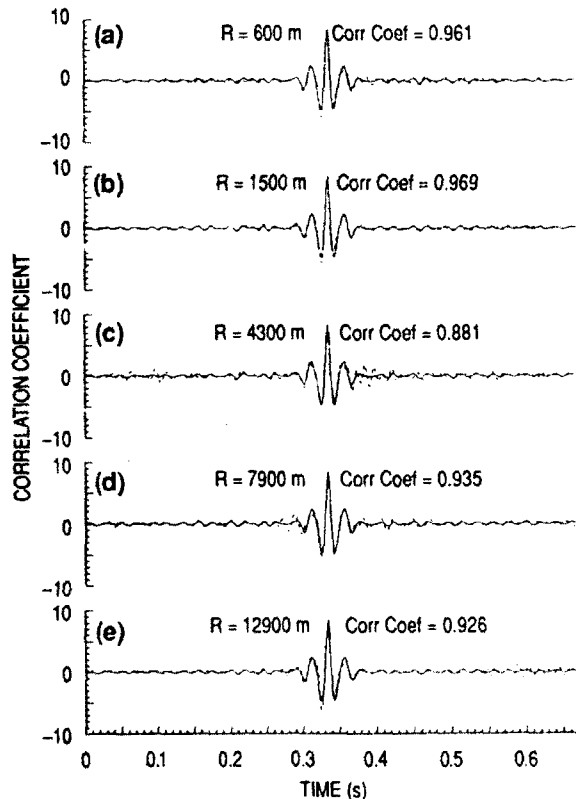


FIG. 13. Comparison of source signature (solid) with source estimates (dashed) obtained from deconvolving measurements with optimized Green's functions ($\beta=29$) for the five ranges considered.

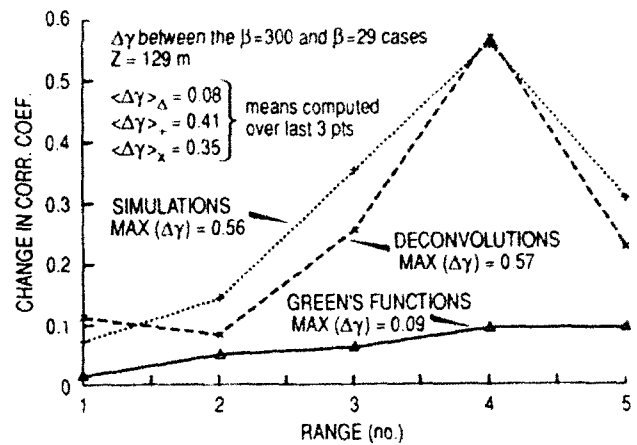


FIG. 14. The change in correlation coefficients between $\beta=300$ (model) and $\beta=29$ for (1) the Green's functions (+), and the simulations (x) for the five ranges considered (numbered 1-5 as range increases). The means are over the last three ranges.

for the curves in Fig. 14. The averages over the last three ranges are $\langle\Delta\gamma\rangle_{GF}=0.08$, $\langle\Delta\gamma\rangle_{SIM}=0.41$, and $\langle\Delta\gamma\rangle_{DCN}=0.35$, and the maxima can be written $\text{Max}(\Delta\gamma) = \{0.09 \text{ (GF)}, 0.56 \text{ (SIM)}, 0.57 \text{ (DCN)}\}$. This indicates that relatively large changes ($\Delta\gamma \sim 0.6$) in the simulation and source estimate quality can be caused by relatively small perturbations ($\Delta\gamma \sim 0.1$) to the corresponding Green's functions when multipath is significant.

VII. CONCLUSIONS

We have shown a sensitivity of the acoustic transients deconvolution problem to small errors in the Green's function when the multipath structure is sufficiently complex. Our multipath is mainly due to interaction with the sediment layers in the bottom, which is where we have the least information. We conclude that, in this kind of scenario, estimates of accuracy requirements in the environmental parameters (especially the subbottom) and in the source location should be an important part of any deconvolution scheme involving multipath (especially bottom interacting). We reiterate that the well-known sensitivity due to the ill-posed nature of the problem is a different effect. It consists of small changes to the data d causing large changes to the source estimate s_e . We have dealt with this problem by replacing the original ill-posed problem with a well-posed extension (in the Tikhonov sense). Furthermore, the simulations (see Fig. 14) show a similar sensitivity to the deconvolutions. The simulations were produced by convolution, a well-posed mathematical operation.

ACKNOWLEDGMENTS

This work was supported by the Office of Naval Research funded Acoustic Transients ARI, program element number 0601153N, under Naval Research Laboratory (Stennis Space Center) program management (Dr. Edward Franchi). NRL Contribution No. JA 244:064:92. We would like to extend thanks to the anonymous reviewer for

several important suggestions affecting the overall quality of the manuscript. We would also like to thank Dr. George Ioup of the University of New Orleans, New Orleans, Louisiana for reading corrections and making helpful suggestions. We would also like to acknowledge the contributions of Mr. E. J. Yoerger of NRL-SSC in the data acquisition phase of this project.

¹A. N. Tikhonov and V. Y. Arsenin, *Solutions of Ill-Posed Problems*, translation edited by F. John (V Winston, Washington, DC, 1977).
²A. Tarantola, *Inverse Problem Theory: Methods for Data Fitting and Model Parameter Estimation* (Elsevier, New York, 1987).
³R. L. Field and J. H. Leclere, "Measurements of Bottom-Limited Ocean Impulse Responses and Comparisons with the Time Domain Parabolic Equation," *J. Acoust. Soc. Am.* **93**, 2599-2616 (1993).
⁴M. D. Collins, "The Time-Domain Solution of the Wide-Angle Parabolic Equation including the Effects of Sediment Dispersion," *J. Acoust. Soc. Am.* **84**, 2114-2125 (1988).
⁵M. D. Collins, "Applications and Time-Domain Solution of Higher-

Order Parabolic Equations in Underwater Acoustics," *J. Acoust. Soc. Am.* **86**, 1097-1102 (1989).
⁶A. Tikhonov, "Regularization of Incorrectly Posed Problems," *Sov. Math.* **4**, 1624-1627 (1963).
⁷R. J. O'Dowd, "Ill-Conditioning and Pre-Whitening in Seismic Deconvolution," *Geophys. J. Int.* **101**, 489-491 (1990).
⁸S. Treitel and L. R. Lines, "Linear Inverse Theory and Deconvolution," *Geophysics* **47**, 1153-1159 (1982).
⁹S. Treitel and R. J. Wang, "The Determination of Digital Wiener Filters from an Ill-Conditioned System of Normal Equations," *Geophys. Prosp.* **24**, 317-327 (1976).
¹⁰P. C. Hansen, "Numerical Tools for Analysis and Solution of Fredholm Integral Equations of the First Kind," *Inverse Problems* **8**, 849-872 (1992).
¹¹J. F. Claerbout, *Fundamentals of Geophysical Data Processing* (McGraw-Hill, New York, 1976).
¹²N. Levinson, "The Wiener RMS (Root Mean Square) Error Criterion in Filter Design and Prediction," *J. Math. Phys.* **25**, 261-278 (1946).
¹³E. A. Robinson, *Multichannel Time Series Analysis* (Holden-Day, San Francisco, 1967) rev. ed.
¹⁴L. E. Scales, *Introduction to Non-Linear Optimization* (Springer-Verlag, New York, 1985).

UNCLASSIFIED UNINSPECTED

Accession For	
NTIS GRA&I	<input checked="" type="checkbox"/>
DTIC TAB	<input type="checkbox"/>
Unannounced	<input type="checkbox"/>
Justification	
By _____	
Distribution/	
Availability Codes	
Dist	Avail and/or Special
A-1	20